



High-resolution mapping of monthly industrial water withdrawal in China from 1965 to 2020

Chengcheng Hou^{1,2}, Yan Li^{1,2,*}, Shan Sang^{1,2}, Xu Zhao³, Yanxu Liu^{1,2}, Yinglu Liu^{4,5}, Fang Zhao⁶

¹Institute of Land Surface System and Sustainable Development, Faculty of Geographical Science, Beijing Normal University, Beijing, 100875, China

²State Key Laboratory of Earth Surface Processes and Resources Ecology, Beijing Normal University, Beijing, 100875, China

³Institute of Blue and Green Development, Shandong University, Weihai, 264209, China

⁴College of Urban and Environmental Sciences, Peking University, Beijing, 100871, China

⁵Key Laboratory for Earth Surface Processes of the Ministry of Education, Peking University, Beijing, 100871, China

⁶Key Laboratory of Geographic Information Science of the Ministry of Education, School of Geographic Sciences, East China Normal University, Shanghai 200241, China.

Correspondence to: Yan Li (yanli.geo@gmail.com)

Abstract. High-quality gridded data on industrial water use is vital for research and water resource management. However, such data in China usually have low accuracy. In this study, we developed a gridded dataset of monthly industrial water withdrawal (IWW) for China, namely, the China industrial water withdrawal dataset (CIWW), which spans a 56-year period from 1965 to 2020 at a spatial resolution of 0.1° and 0.25°. We utilized >400,000 records of industrial enterprises, monthly industrial product output data, continuous statistical IWW records from 1965 to 2020, to facilitate spatial scaling, seasonal allocation, and long-term temporal coverage in the developing the dataset. The CIWW dataset presented significant improvement in characterizing the spatial and seasonal patterns of IWW dynamics in China, with a much higher accuracy at fine scale while ensuring consistency with statistical records. The CIWW dataset, together with its methodology, and auxiliary data, is useful for water resource management and for research in hydrology, geography, environment, and sustainability sciences. This new dataset is now available at <https://doi.org/10.6084/m9.figshare.21901074.v1> (Hou and Li, 2023).

1 Introduction

Industrial water withdrawal (IWW) accounted for approximately 19% of human water withdrawal globally, which is the second largest sector of human water use following irrigation (WWAP, 2019). In developed countries, IWW accounted for more than half of their water use (Shen et al., 2010; Wada et al., 2011a; Flörke et al., 2013). Driven by economic and population growth, global IWW has steadily increased over the past 60 years (Oki and Kanae, 2006; Wada et al., 2011b) from 400 km³ per year in 1960 to 955 km³ per year in 2010 (Flörke et al., 2013) and it was projected to continue to increase in the future (Oki et al., 2003; Shen et al., 2010; Fujimori et al., 2017). Considering the high spatial heterogeneity and fast changes of IWW, quantitative information with high spatiotemporal resolution on IWW is essential for water resource management and research.



Existing data of IWW primarily consisted of statistical data at administrative or watershed levels and model estimations at the grid level, in which the sectoral information was represented with varying details (Arnell, 1999, 2004; Alcamo et al., 2000, 2007; Vörösmarty et al., 2000; Oki et al., 2003; Hanasaki et al., 2008a; OTAKI et al., 2008; Wada et al., 2011b; Hejazi et al., 2014; Wada et al., 2016; Yan et al., 2022). However, these datasets have their limitations. Although gridded data, typically developed from administrative-level, emerged to provide more detailed spatial information (Hanasaki et al., 2008a; Wada et al., 2011a), their accuracy depended on the downscaling methods. For the total IWW, statistics were usually allocated to grids level relying on spatial proxies such as population density, urban or industrial area (Hanasaki et al., 2008a, b, 2010; Beek et al., 2011; Wada et al., 2011a, b, 2014). For sectoral IWW, different mapping methods were applied. Water withdrawal for energy sector was estimated by the total energy generated and water use efficiency under different technologies (Koch and Vögele, 2009; Flörke et al., 2013). With detailed information on the location, power output, and water use efficiency of power plants, water withdrawal for energy sector could be mapped out (Vassolo and Döll, 2005; Flörke et al., 2013; Müller Schmied et al., 2014; Wang et al., 2016; Qin et al., 2019). Water withdrawal for manufacturing was estimated either as the residue of energy water use from the total IWW (Hejazi et al., 2014) or product of population and per capita water consumption (Vörösmarty et al., 2000). Although several global gridded IWW datasets have been developed using these methods, how well spatial proxies such as population can represent the spatial distribution of IWW is unclear (Otaki et al., 2008). Moreover, the coarse resolution (e.g., 0.5°) and low accuracy of global datasets, especially at fine scale, limit their applications for regional water issues.

IWW had seasonal fluctuations because of changes in weather conditions (temperature, precipitation, thunderstorms), water supply availability (especially under monsoon climates such as in China), production demand, and emission restrictions (Liu et al., 2006). However, most existing datasets either neglected seasonal variations or simply treating them as invariable across months (i.e., each month shared 1/12 of annual total withdrawal) (Brunner et al., 2019; Wada et al., 2011a). These misrepresented intra-annual variations may result in significant discrepancies between the data and reality. In a few studies, seasonal variations in water withdrawal were considered for specific sectors. For example, seasonality in water withdrawal for electricity generation was considered by incorporating the influence of temperature variability on the cooling water demand of thermoelectric power plants (Byers et al., 2014; Liu et al., 2015). Results demonstrated a clear seasonal pattern, with large withdrawals in winter at high-latitudes and summer in tropical regions (Huang et al., 2018). Therefore, it is essential to fully account for intra-annual variations in IWW, which directly affect water resource management and allocation (Derepasko et al., 2021; Sunkara and Singh, 2022).

After decades of fast growth, China has become the second-largest economy in the world, with the rapid industrial development leading to increasing water use (Zhou et al., 2020). Industrial water withdrawal in China accounted for 20.2% of total water withdrawal in 2019 (source: China water resources bulletin) and increased by 4.5 times from 31.93 km^3 in 1965 to 142.86 km^3 in 2013 (Zhou et al., 2020). However, water resources in China are spatially distributed unevenly, causing severe water stress due to mismatch between water supply and demand from population and industrial development (Liu et al., 2013; Zhao et al., 2015). For instance, Northern China, one of China's largest industrial centres and densely populated region, is one of the most



65 water scarce in the world (Yin et al., 2020). The growth in water demand has further increased the water conflict, making it
urgent to optimize current water use and management structure and prepare for future climate change. However, IWW data
produced from reliable data sources with a long period and high spatial resolution in China is still lacking. The publicly
available data of IWW in China are either statistical data at provincial, prefecture, or basin level (Xia et al., 2017; Qin et al.,
2020; Chen et al., 2021), or gridded data extracted from global datasets which have poor regional accuracy (Liu et al., 2019a,
70 b; Han et al., 2019; Niva et al., 2020; Yin et al., 2020; Li et al., 2022).

To fill this data gap, in this study, we were motivated to use reliable local data sources to develop gridded datasets of monthly
IWW in China with high spatial resolution and seasonal variations. By using multiple statistical data, the high-resolution
mapping of IWW was achieved by a unique industrial enterprises dataset including >400,000 enterprises; the seasonal
variations were derived from industry product output data; and the long-term temporal coverage was obtained by continuous
75 statistical records from 1965 to 2020. The resulting dataset, named the China Industrial Water Withdrawal dataset (CIWW),
provides monthly IWW from 1965 to 2020 at a spatial resolution of 0.1° and 0.25°. The dataset would be useful to better
understand the spatial and seasonal variations of IWW in China and support hydrological studies and regional water resource
management.

2 Data and Method

80 In this study, IWW was defined as the amount of water abstracted from freshwater sources for industrial rather than water
consumption.

2.1 Data

2.1.1 Statistical data for industrial output value and water withdrawal

The provincial-level industrial output value (IOV, unit: 10³ Yuan per year) and IWW were from the Chinese Economic Census
85 Yearbook in 2008 (<http://www.stats.gov.cn/tjsj/pcsj/jjpc/2jp/left.htm>, last access: 2 April 2021). The data included
surveyed IOV and IWW for enterprises above a designated production level, consisting of three main industrial sectors (mining,
manufacturing, and production and supply of electricity, gas and water) and 38 subsectors (Table A1). Note that two subsectors
“Other Mining” and “Waste Resources and Material Recycling and Processing” had no data, we used the averaged IOV and
IWW value of the mining and manufacturing sector in each province to fill these two subsectors.

90 2.1.2 Industrial enterprise data in China

The industrial enterprise dataset used in this study was from the Database of Chinese Industrial Enterprises in Mainland China
from 1998 to 2013 (<https://www.lib.pku.edu.cn/portal/cn/news/0000001637>, last access: 18 May 2022). The datasets
contained industrial information such as address, products, annual IOV, and industry category for more than 400,000



enterprises whose IOV was more than 5 million Yuan (or 20 million Yuan from 2011 to 2013 due to standard changes). The dataset covered three main industrial sectors and 37 subsectors, similar to the provincial statistical data. The enterprises' records for subsector 'Water Production and Supply' were not used because the water supply was mainly for domestic rather than industrial purposes. To match the surveyed IWW data, which were only available in 2008, industrial enterprise data in 2008 were selected for spatial downscaling the provincial IWW (Fig. B2).

2.1.3 Statistical data for monthly industrial product output

The monthly industrial product output data were from the China Industry Product Output Database (http://olap.epsnet.com.cn/auth/platform.html?sid=9C98BFB19A412FF66F744C2DA364ED5E_ipv473399501&cubeId=52, last access: 26 September 2021). The data contained monthly outputs of 283 specific products of 36 industrial subsectors at the provincial level. We used the average of 5 years from 2006-2010 to reduce interannual variability in outputs. The monthly output of each product was converted to monthly fractions (divided by the annual total output) to represent its intra-annual variation. Missing values in monthly product output fractions were filled by the average value of monthly fractions of product output from 2006 to 2010. The monthly output fractions of 283 products were aggregated to 36 subsectors by averaging products within each subsector by arithmetic mean.

2.1.4 Statistical data for water use to extend long-term water withdrawal data

In order to produce IWW data for the past four decades, long time statistical IWW data were required. Provincial statistical data on industrial water use in China from the National Water Resources Bulletin (<http://www.mwr.gov.cn/sj/tjgb/szygb/>, last access: 3 May 2022) from 2003 to 2020 was used. To further extend the time series to the earlier period, the industrial water use by Zhou et al., 2020 (referred to as 'Zhou2020 data' hereafter) from 1965 to 2002 was used by summing up the prefecture data to the provincial level. Noting that IWW and industrial water use (i.e., the annual quantity of water withdrawal for industrial purposes) were treated the same in our study due to their similar definition, allowing us to obtain complete statistical records of IWW from 1965 to 2020 in China.

Table 1 provides a summary of source data for developing CIWW dataset.

Table 1 A summary of source data for developing CIWW

Data	Data Source	Industrial Sector	Spatial resolution	Time span	Purpose
Industrial enterprise output value	Database of Chinese Industrial Enterprises	Subsectors	Point	Yearly, 2008	Spatial downscaling
Industrial water withdrawal	Chinese Economic Census Yearbook	(36)	Province	Yearly, 2008	



Industrial output value					
Monthly product output (283 products)	China Industry Product Output Database		Province	Monthly, 2006-2010	Seasonal allocation
Industrial water use	China National Water Resources Bulletin	None	Province	Yearly, 2003-2020	Long-term data from 1965 to 2020
Industrial water use	Zhou et al., 2020	Sectors (10)	Prefecture	Yearly, 1965-2002	

2.2 Method

The development of the CIWW dataset primarily consisted of three steps: 1) spatial mapping of provincial IWW data to grid-
 120 scale, 2) seasonal allocation of annual IWW data to monthly scale, and 3) production of long time series of IWW (Fig. 1).

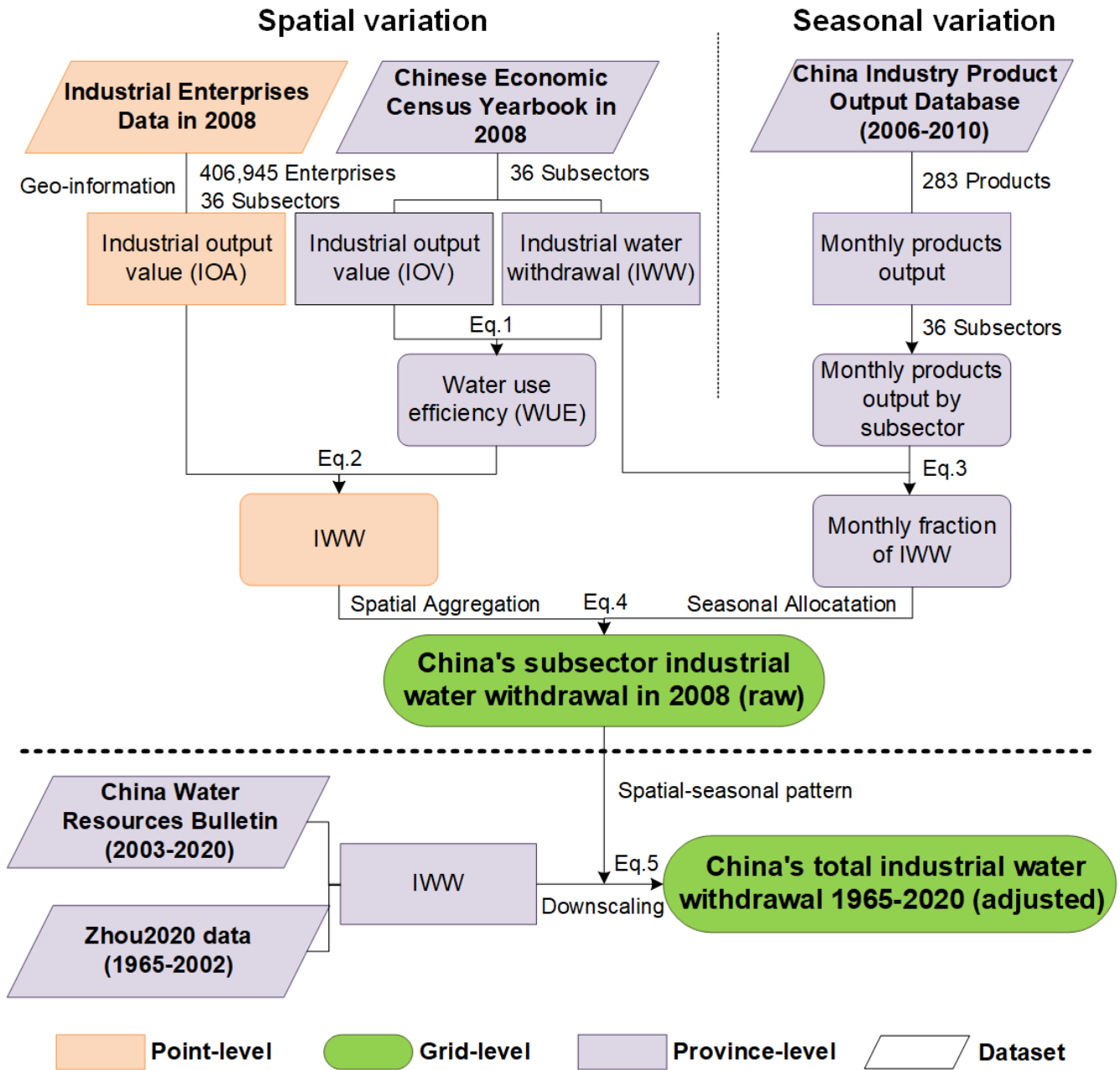


Figure 1: The workflow for developing the CIWW dataset.

2.2.1 Mapping industrial water withdrawal

The spatial mapping of IWW in China was achieved using the IOV of >400,000 enterprises in 2008 and the sub-sectoral water use efficiency at the provincial level from the Chinese Economic Census Yearbook in 2008.



The geographical location of industrial enterprises was obtained by converting their addresses to geographical coordinates by the BaiduV3 geocoding service with the *geopy* package in python. The industrial water use efficiency ($WUE_{p,subs}$) of province p and subsectors $subs$ was computed as industrial output value ($IOV_{p,subs}$) divided by industrial water withdrawal ($IWW_{p,subs}$) (Eq. (1)):

$$130 \quad WUE_{p,subs} = \frac{IOV_{p,subs}}{IWW_{p,subs}} \quad (1)$$

By assuming industrial water use efficiency was the same for all industrial enterprises in the same province and the same subsector, industrial water withdrawal ($IWW_{i,subs}$) of enterprise i belonging to subsector $subs$ was estimated by multiplying the corresponding water use efficiency of subsector $subs$ in province p ($WUE_{p,subs}$) and the industrial output value of enterprise i ($IOV_{i,subs}$) as Eq. (2):

$$135 \quad IWW_{i,subs} = WUE_{p,subs} \times IOV_{i,subs} \quad (2)$$

The IWW of each enterprise of the same subsectors ($IWW_{i,subs}$) could be summed up from the point level to the grid level at a given resolution ($IWW_{grid,subs}$). Summing through subsectors ($\sum_{subs=1}^{36} IWW_{grid,subs}$) gave the spatial pattern of the total IWW in 2008.

2.2.2 Allocating industrial water withdrawal to seasonal variations

140 We assumed that IWW was proportional to industrial product output with a constant water use efficiency during the year at the monthly scale. Therefore, seasonal variations in IWW could be approximated by seasonal variations in industrial product output, which were calculated as the monthly fractions of product output to annual total output.

Since the monthly industrial product output data included 283 different products of different subsectors and the number of products varied across subsectors, we first calculated the monthly fraction of each product output of each province, averaged
145 from 2006 to 2010, to reduce the influence of inter-annual variability. Because water use for producing different products was unknown, we simply used arithmetic mean of different products to represent aggregated monthly fractions for each subsector. By this way we obtained fractions of product outputs for subsector $subs$, in province p for month mon ($Fraction_{p,mon,subs}^{output}$).

We found $Fraction_{mon,p,subs}^{output}$ in certain subsector and provinces exhibited unreasonable seasonal variations which were hard to explain. Instead of directly using the provincial-specific seasonal variations of output, we calculated seasonal variations of
150 each industrial subsector ($Fraction_{mon,subs}^{water}$) through the weighted mean of monthly product fractions across all provinces ($Fraction_{mon,p,subs}^{output}$) with weights of provincial subsector IWW ($IWW_{p,subs}$) from Chinese Economic Census Yearbook in 2008 (Eq. (3)).

$$Fraction_{mon,subs}^{water} = \frac{\sum_{p=1}^{31} (Fraction_{p,mon,subs}^{output} \times IWW_{p,subs})}{\sum_{p=1}^{31} IWW_{p,subs}} \quad (3)$$



Therefore, the monthly IWW of different subsectors at grid level ($IWW_{grid,mon,subs}$) could be obtained by allocating its annual
 155 IWW ($IWW_{grid,subs}$) into 12 months based on the corresponding monthly fractions of the same subsector ($Fraction_{mon,subs}^{water}$)
 as Eq. (4).

$$IWW_{grid,mon,subs} = IWW_{grid,subs} \times Fraction_{mon,subs}^{water} \quad (4)$$

The monthly IWW at grid level ($IWW_{grid,mon}$) after summing subsectors ($\sum_{subs=1}^{36} IWW_{grid,mon,subs}$) gave the spatial and
 seasonal pattern of the total IWW of China in 2008.

160 2.2.3 Developing China's industrial water withdrawal data from 1965 to 2020

We developed long-term IWW data in China from 1965 to 2020 by mapping provincial IWW statistics in other years based
 on the spatial-seasonal pattern derived from IWW in 2008. Due to statistical differences in data sources, the raw IWW from
 the 2008 Chinese Economic Census Yearbook was not directly used in developing the long-term data. Instead, its spatial-
 seasonal distribution was used to map the provincial industrial water withdrawal (IWW_p) from China National Water
 165 Resources Bulletin between 2003 and 2020 and Zhou2020 data between 1965 and 2002. Since Zhou2020 data showed good
 consistency with the China Water Resources Bulletin data, these two IWW records were combined to develop long-term data.
 The provincial industrial water withdrawal (IWW_p) of each year was allocated to the grid level following Eq. (5) to obtain the
 gridded IWW data from 1965 to 2020 ($IWW_{grid,mon}^{adjust}$):

$$IWW_{grid,mon}^{adjust} = IWW_p \times \frac{IWW_{grid,mon}^{raw}}{\sum_p \sum_{mon=1}^{12} IWW_{grid,mon}^{raw}} \quad (5)$$

170 where $IWW_{grid,mon}^{adjust}$ was the adjusted IWW of month mon at the grid level, $IWW_{grid,mon}^{raw}$ was the monthly IWW at the grid
 level in 2008, and $\sum_p \sum_{mon=1}^{12} IWW_{grid,mon}^{raw}$ summed the monthly gridded $IWW_{grid,mon}^{raw}$ to annual total IWW of all grids in
 province p .

Table 2 provides an overview of the CIWW dataset, including the gridded monthly IWW data in China from January 1965 to
 December 2020 with a spatial resolution of 0.1° and 0.25° and auxiliary data supporting the development.

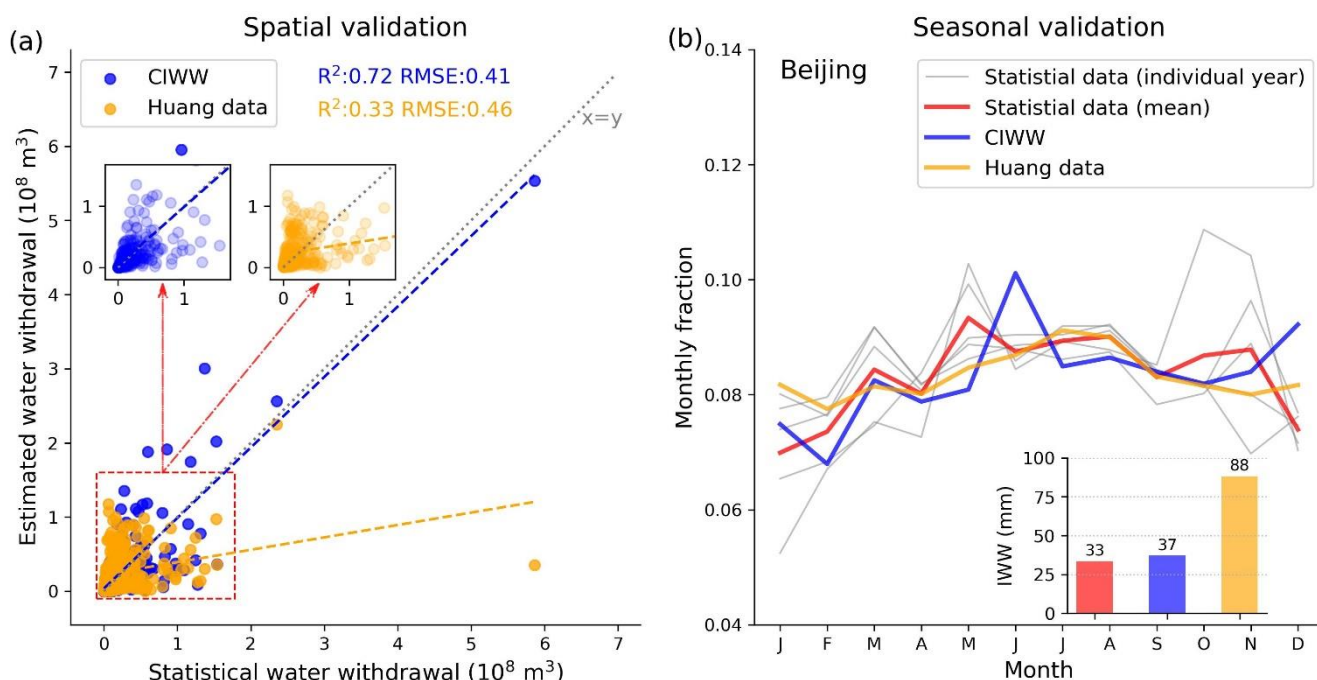
175 **Table 2 Overview of the China Industrial Water Withdrawal (CIWW) Dataset^a**

Data	Variable	Spatial resolution	Temporal coverage	Industrial sectors
Main data	Industrial water withdrawal (adjusted)	$0.1^\circ/0.25^\circ$	Monthly, 1965-2020	NA
	Industrial water withdrawal (raw)	$0.1^\circ/0.25^\circ$	Monthly, 2008	36 subsectors
Auxiliary data	Industrial output value	$0.1^\circ/0.25^\circ$	Yearly, 2008	36 subsectors
	Number of industrial enterprises	$0.1^\circ/0.25^\circ$	Yearly, 2008	36 subsectors

^aThis dataset is available at <https://doi.org/10.6084/m9.figshare.21901074.v1>.



2.3 Validation and comparison with other datasets



180 **Figure 2: Validation of CIWW data against statistical data for spatial distribution and seasonal variation. (a) The relationship**
between the mean IWW of 1971-2010 from statistical data (Zhou et al., 2020) and CIWW and Huang2018 data (Huang et al., 2018)
for 289 cities in China. The grey dotted line indicates the 1:1 line, and the colored dashed lines indicate the fitted lines. (b) The
comparison of the 5-year mean (2006-2010) monthly variation in IWW from statistical data (red, (Long et al., 2020)), CIWW (blue),
and Huang2018 data (green) in Beijing. The solid grey line shows IWW for individual years from 2006 to 2010. The inset shows the
 185 **annual mean total IWW from 2006 to 2010. For this comparison, CIWW was processed to the same spatial resolution of Huang2018**
data at 0.5°.

To validate the performance of the CIWW dataset, we compared the spatial and seasonal patterns with statistical data records and other datasets. For spatial validation, the 40-year mean IWW (1971-2010) from CIWW and other global gridded data (Huang et al., 2018) (referred to as Huang2018 data) were compared with statistical data (Zhou et al., 2020) for 289 cities in China. We used the statistical data at the provincial level to produce the CIWW dataset and the prefecture level to verify the product. The validation at the prefecture level demonstrated how well the spatial patterns were after downscaling. Results in Fig. 2a) indicated a superior performance of CIWW data in representing the spatial variations of IWW compared against statistical data, showing a much higher R^2 (0.72 and 0.33) and lower RMSE (Root Mean Square Error) (0.41 vs. 0.46 $10^8 m^3$) than Huang2018 data. Additionally, annual IWW in China from Huang2018 data were overestimated by 20%~10% from 2005 to 2010 and over 20% from 1999 to 2002 compared to statistical data.

195 For seasonal validation, owing to the data limitation, we only had monthly statistical IWW data in Beijing from 2006 to 2010 (Long et al., 2020). Results showed that both CIWW and Huang2018 data could capture the 5-year mean seasonality of IWW in Beijing. However, the magnitude of IWW was significantly overestimated by Huang2018 data (88 mm per year) relative to

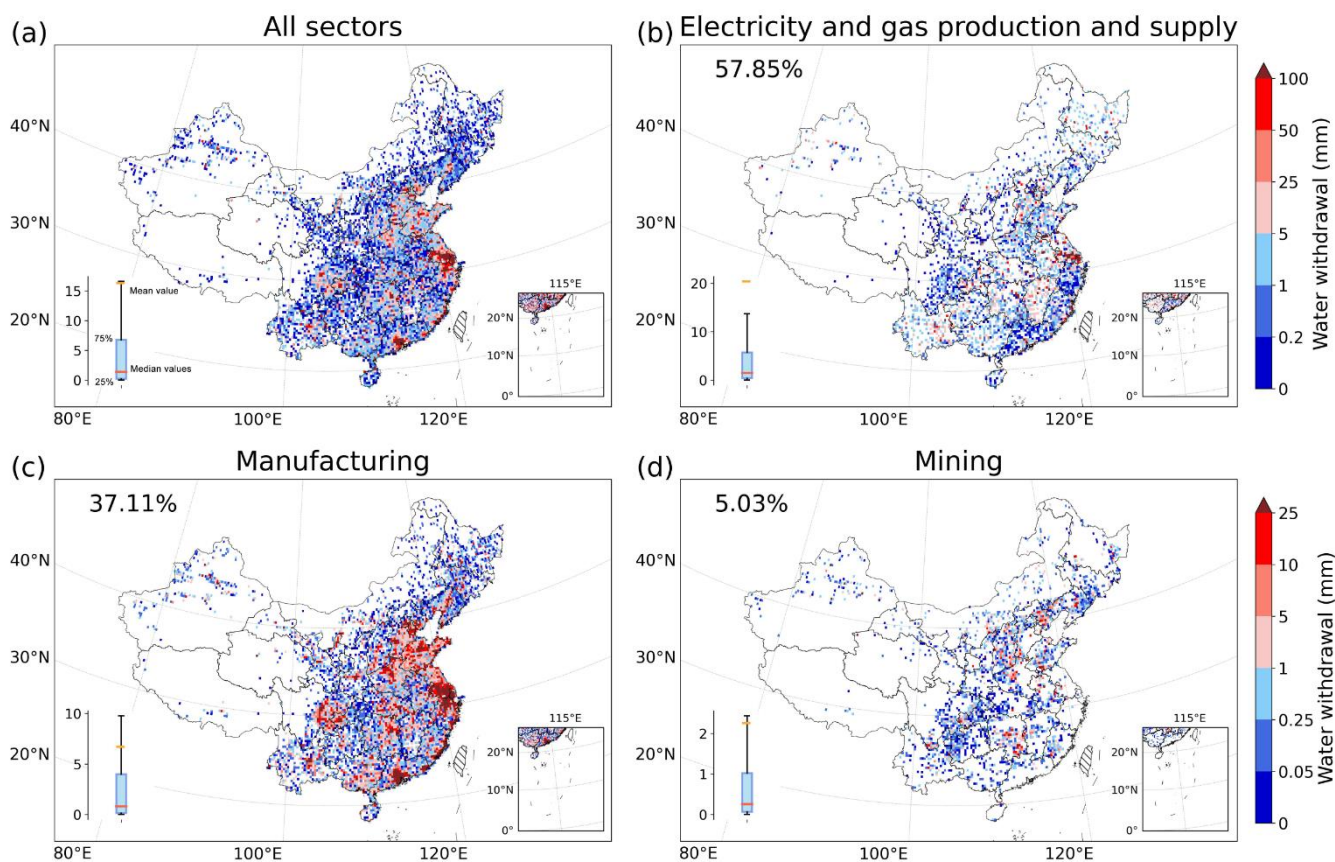


statistical data (33 mm per year). In comparison, the magnitude of IWW in CIWW data (37 mm per year) was more in line with statistical data (Fig. 2b).

200 These validations demonstrated better performance of CIWW data with much higher accuracy and improved representations of spatial and seasonal variations, making it a better data source for IWW related applications in China.

3 Results

3.1 Spatial distribution of industrial water withdrawal in China



205 **Figure 3: The total IWW (raw) in China in 2008 (a) and for different industrial sectors, including electricity and gas production and supply (EGPS, b), manufacturing (c), and mining (d). The box plot in the bottom left corner shows the interquartile range (25% and 75%) of non-zero water withdrawal, with red and yellow lines denoting the median and mean values. Numbers displayed in percentage denote the percentage of the sectoral IWW to total IWW.**

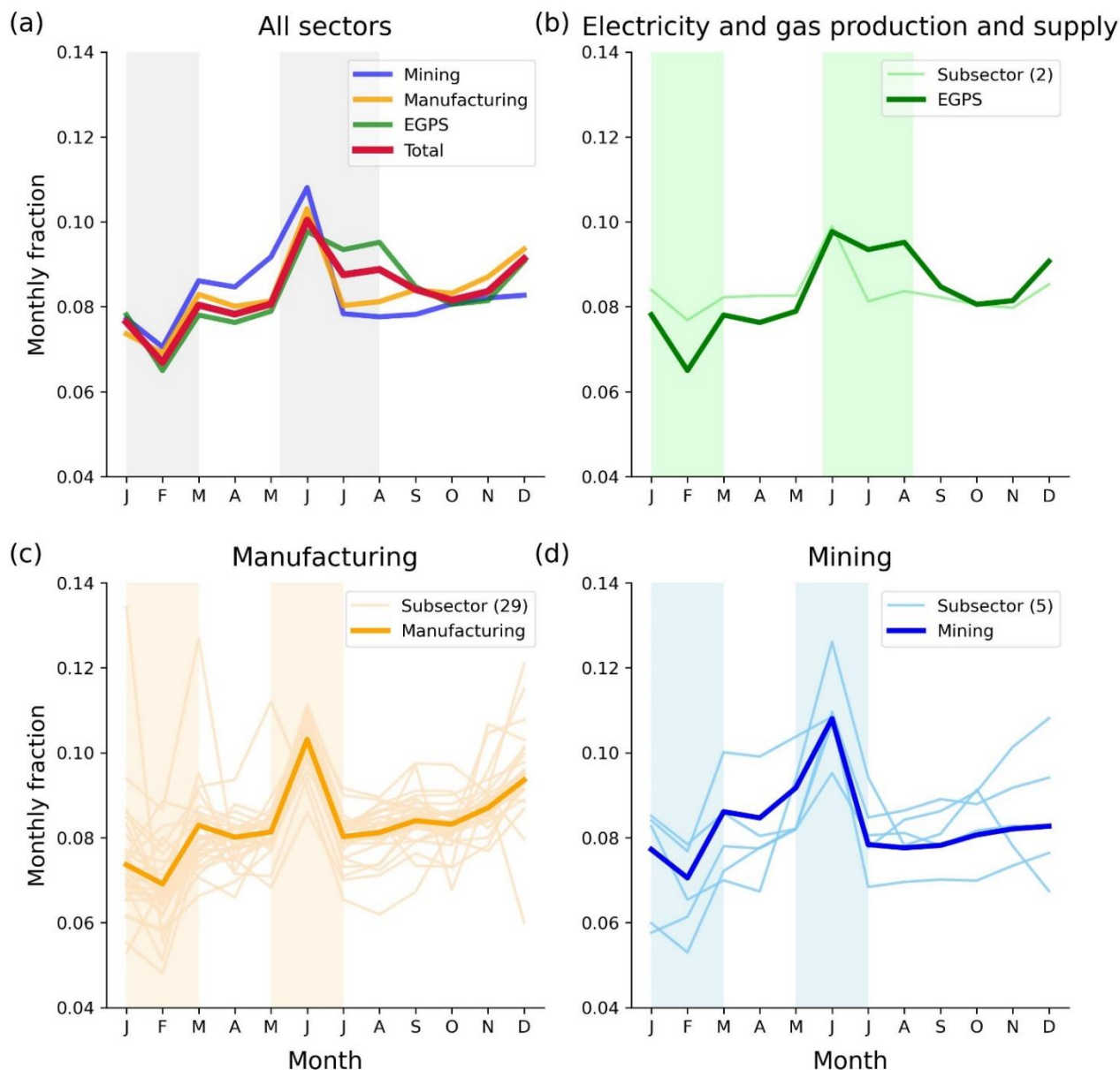
There was substantial spatial variation in total IWW (Fig. 3a). Eastern coastal area of China had generally higher IWW, followed by southeastern and central China, while western China had the least IWW. The largest water withdrawal can be found in the urban agglomeration of the Yangtze River Delta and Pearl River Delta. The spatial distribution of IWW over the country implied that industry enterprises were primarily concentrated in urban area with more intensified economic activities.



215 The water withdrawal by main industrial sectors showed distinctive spatial patterns. Water withdrawal from EGPS expressed a dispersive pattern which was mainly concentrated in southeastern coastal areas, especially in the Yangtze River Delta region (Fig. 3b). Water withdrawal from manufacturing broadly resembled the total IWW and population distribution of China, mainly reflecting the fact that manufacturing and population were closely linked with each other (Fig. 3c). Water withdrawal of mining was confined to regions with rich mineral resources such as the central, northern, and southwestern China (Fig. 3d). Overall, the sector with the largest IWW was EGPS (57.85%), followed by manufacturing (37.11%) and mining (5.03%). The dominance of the EGPS sector in total IWW reflected the large water requirement for thermoelectric power generation (Gu et al., 2016; Niva et al., 2020).
220



3.2 Seasonal variations of industrial water withdrawal in China



225

Figure 4: The seasonal variations of the national total IWW (a) and for separate industrial sectors, including electricity and gas production and supply (EGPS) (b), manufacturing (c), and mining sectors (d). The seasonal variations were represented as the fraction of monthly IWW to the annual total during 2006-2010. The thick lines stand for water withdrawal of main industrial sectors, and the thin color lines stand for subsectors. Shadows represent the seasons with peak and low water withdrawal of a year.

The seasonal variations of IWW during 2006-2010, represented by the fraction of monthly water withdrawal to annual total, are shown in Fig. 4. Results suggested that the IWW peaked in summer (June to August, 28%), followed by autumn (September



to November, 25%), spring (March to May, 24%) and winter (December to February, 23%) (Fig. 4). February was the month
230 with the lowest IWW, possibly due to its fewer days and the coincidence with the Chinese Spring Festival holiday (Liu et al.,
2006). The highest IWW occurred in June, probably due to the largest industrial output and high demand for cooling. Such an
IWW peak did not extend to other summer months because extreme weather events such as heat waves and heavy rain occurred
more frequently in July and August, resulting in production shutdowns and reduced water consumption (Liu et al., 2006).
Seasonal patterns of IWW for manufacturing and mining sectors were generally similar, but the subsectors of manufacturing
235 showed more diverse patterns. IWW for EGPS had quite different seasonality, as there were two peaks in June to August and
December, which probably reflected the seasonal changes in cooling water withdrawal for thermal electricity generation due
to seasonal temperature variation. Summer peak of EGPS was related to the high energy demand for air conditioning cooling
(Huang et al., 2018), and the winter peak was related to the high energy demand for heating (Byers et al., 2014; Liu et al.,
2015; Huang et al., 2018).

240 3.3 Trend of industrial water withdrawal in China from 1965 to 2020

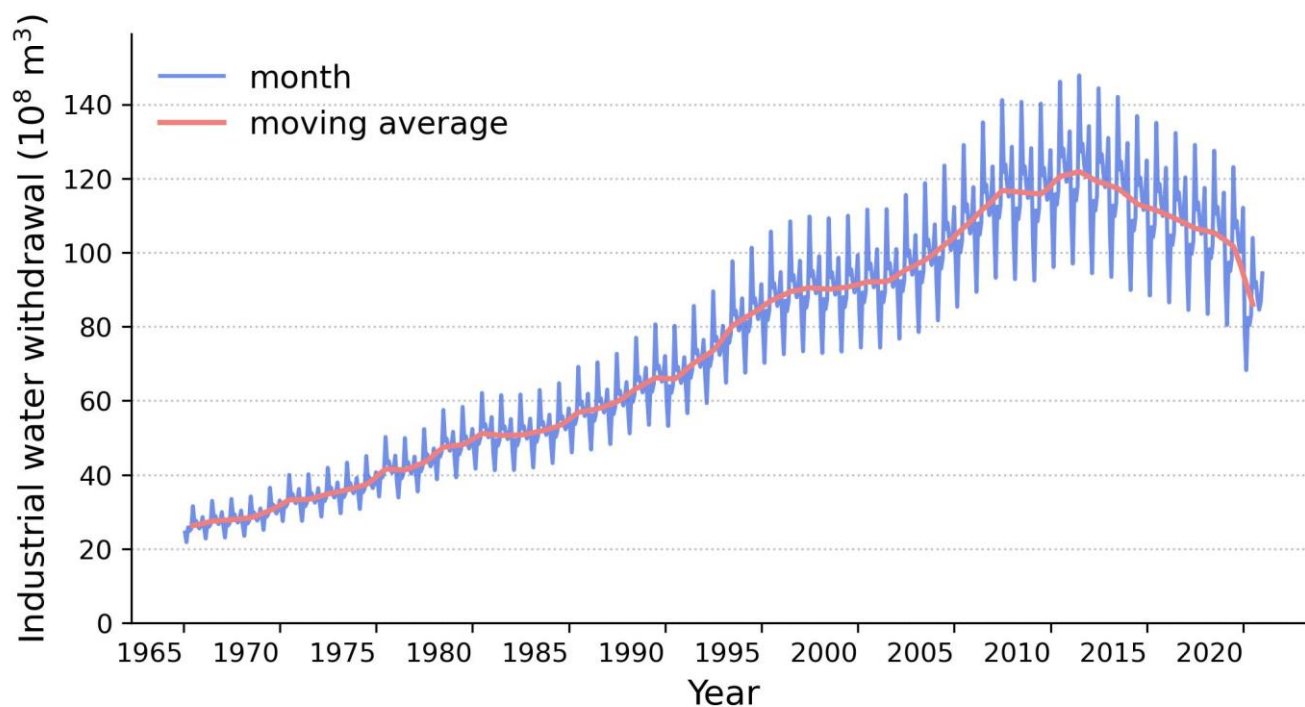


Figure 5: The monthly industrial water withdrawal in China from 1965 to 2020 in the CIWW dataset. The red line represents moving average of monthly IWW of a 12-month moving window.

For interannual monthly variations, IWW in China had increased significantly from 2.1 billion m^3 per month to 14 billion m^3
245 per month during 1965–2010, and it then decreased to 10 billion m^3 per month (Fig. 5). These long-term changes indicated
that IWW in China now has entered a slowly declining phase.



4 Discussion

Our study developed new gridded data for IWW in China from 1965 to 2020. The CIWW dataset improves upon previous data particularly in high spatial and seasonal patterns. Instead of using indirect proxies like population density to map out IWW, we used industrial enterprise data which were direct water withdrawers. Compared with existing IWW data that either lack or only have limited representation of seasonal changes (Wada et al., 2011b; Huang et al., 2018; Brunner et al., 2019), our data presented seasonal variations based on information from direct water consumer: sectorial industrial production processes. Further, we used localized data sources in China to produce the long-term IWW data, significantly improving regional accuracy and consistency with statistical data records. The usage of public data sources and transparent methodology makes it possible to further update and recalibrate the data for specific user needs.

4.1 Potential applications of industrial water withdrawal data: high-resolution analysis and data scaling

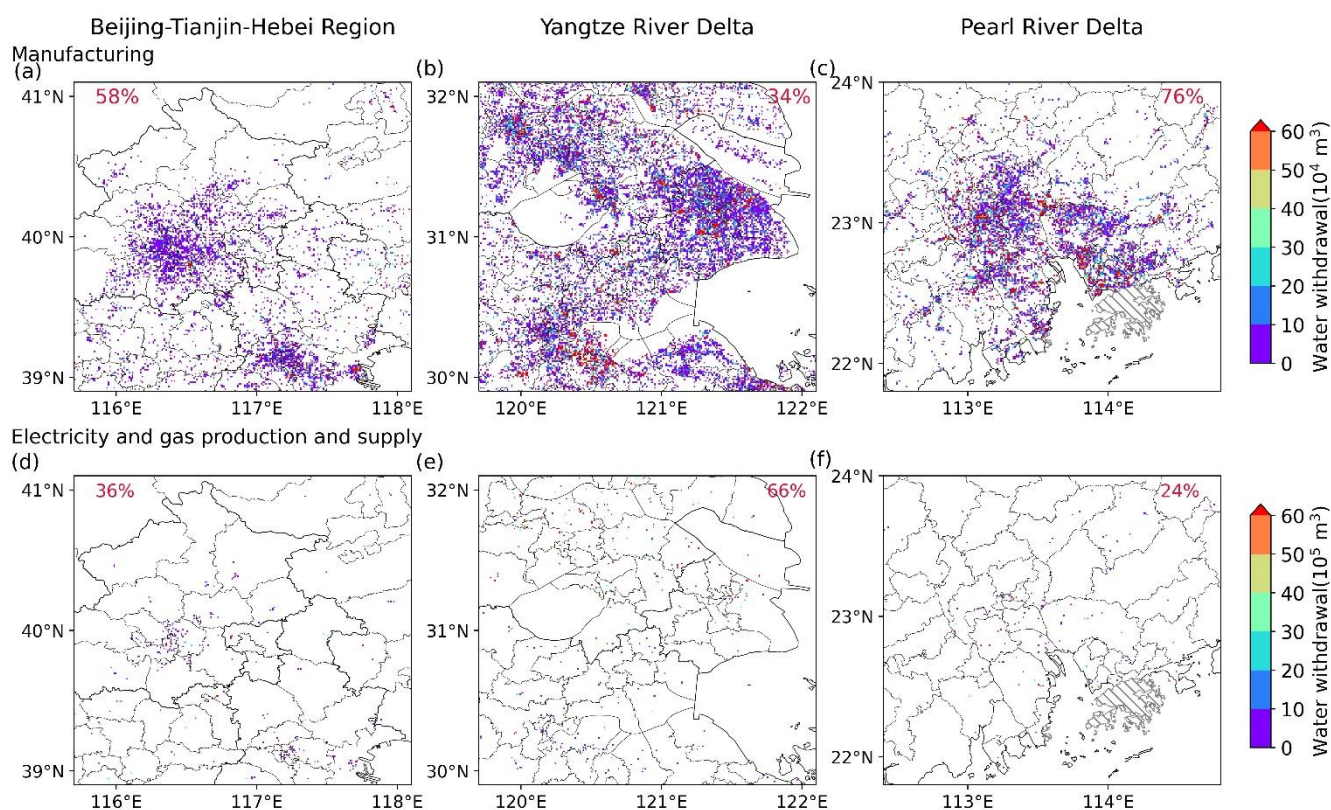


Figure 6: Zoomed view of IWW in densely urbanized regions in China at a spatial resolution of 0.01° , including the Beijing-Tianjin-Hebei region (a, d), Yangtze River Delta (b, e), and Pearl River Delta (c, f). Panels (a)–(c) show IWW for manufacturing, and panels (d)–(f) shows IWW for electricity and gas production and supply. Numbers displayed in percentage denote the percentage of the sectoral IWW to total IWW.



The IWW data product with high resolutions supports various research applications. On the one hand, the high spatial resolution revealed IWW at fine scales. Figure 6 shows IWW hotspots in some of China's most densely urbanized regions in 2008 at 0.01° (this resolution is not included in the CIWW dataset but can be produced by the data and code we provided), including the Beijing-Tianjin-Hebei, the Yangtze River Delta, and Pearl River Delta. These maps displayed high heterogeneity of IWW at local scales.

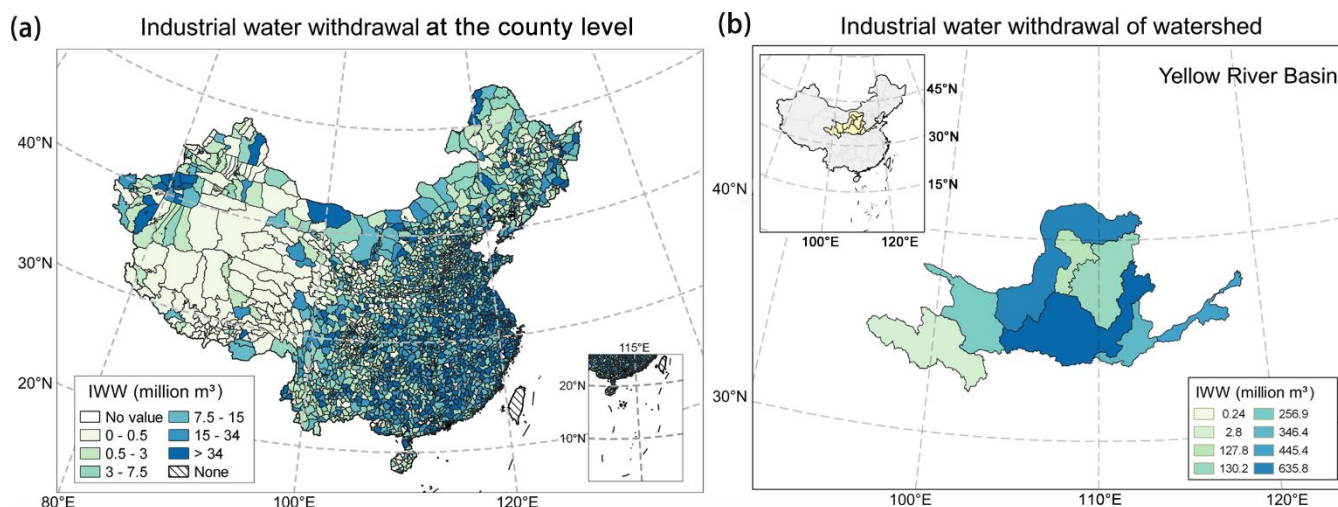


Figure 7: CIWW data facilitate downscaling of IWW from provincial to county levels in China (a) and from provincial to watershed levels in the Yellow River Basin (b).

On the other hand, our data can facilitate downscaling of statistical data between different administrative (e.g., provincial or prefecture level), natural (e.g., watershed), and grid levels and help reconcile the scale mismatch between data with different spatial units (e.g., administrative and watershed/catchment). For example, with the gridded CIWW data, the statistical provincial IWW data could be downscaled to the prefecture-level or even the county level (Fig. 7a). Moreover, the provincial IWW could be scaled to the watershed level using weights from the gridded IWW. Figure 7b shows IWW rescaled from provincial levels to watersheds in the Yellow River basin.

4.2 Uncertainties in spatial downscaling methods

The spatial pattern of IWW in CIWW dataset was primarily based on >400,000 industrial enterprises in 2008. The spatial sampling of industrial enterprises could affect the reliability of spatial mapping. Although this was a large number of records, the enterprise dataset could not cover all industries in China, as it only sampled enterprises above a designated production level. This means other enterprises below this level, including their IWW, would be omitted from the datasets, leading to spatial under-sampling of all industries and their IWW in China. According to the 2008 Chinese Economic Census Yearbook, the enterprises above a designated level accounted for 93% of IOV and 85% of water withdrawal of all industries. This suggested that spatial sampling would have a limited influence on the overall spatial pattern. Also, this issue could be mitigated when point-level enterprise estimates were aggregated to the grid level.



285 Another source of uncertainty comes from water use efficiency. Ideally, the enterprise-level IWW could be estimated using each enterprise's IOV and WUE. However, the enterprise-specific WUE was unavailable, so we used the provincial subsectorial WUE instead to estimate IWW. We assumed that enterprises of the same subsector in the province had similar WUE. In real situation, the WUE of different enterprises may vary substantially depending on subsector and technological levels. The data can be improved with better data sources in future.

290 **4.3 Uncertainties in seasonal allocation methods**

When allocating the annual IWW to monthly scales, we used monthly variations of industrial product output data to represent the seasonal variation of IWW. It should be emphasized that there were differences in monthly variations across different products and provinces. When aggregating the monthly variations of 283 products to subsectors, each product was assigned an equal weight due to the lack of product-specific WUE, which neglected the structural differences within the subsector
295 because products consuming more water should play a more important role in determining the seasonal variation of the subsector. When aggregating IWW from subsector to sector, the structural differences within a sector were considered with the weights of subsector WUE.

We observed considerable differences in monthly variations of production output across provinces. It is difficult to justify whether these different seasonal fluctuations arose from statistical/random errors, unweighted product outputs to subsector, interannual variability (Fig. 2b), or actual regional differences, so we chose to use the national mean monthly variations to represent each subsector to improve the robustness. These monthly subsector variations were then combined with the subsectorial water withdrawal of each grid to derive its seasonal variations in IWW (Eq. (4)). The regional differences in seasonal variations of IWW should be explored further in future studies.

4.4 Uncertainties in producing long-term gridded data

305 A key step in developing the long-term gridded IWW data was to apply the spatial-seasonal pattern of IWW derived in 2008 to other years (due to data constraint). The year 2008 was chosen to match the 2008 Chinese Economic Census Yearbook data which included detailed IWW information. This means that even though the total IWW increased over time with economic development, their spatial pattern and seasonality remained the same in CIWW. We admitted that the time-invariant spatial-seasonal pattern of IWW was a strong assumption and probably not true in reality. Such a time-invariant spatial pattern had
310 been adopted in previous studies based on either a static population density map (Wada et al., 2016) or maps with decadal updates (Huang et al., 2018). Alternative time-varying data sources, such as nightlights, land cover, and population density maps with frequent temporal updates, could provide additional information to better catheterize the temporal changes in the spatial pattern of IWW. To investigate how spatial patterns had changed over time, we re-estimated IWW using enterprise data in 1998. We found that the spatial pattern from the 1998 data was similar to 2008 at 0.25° (the Spearman rank correlation, $\rho=0.84$). The similarity improved further at coarser grids ($\rho=0.91$ at 0.5°) (Fig. C3). Although specific industrial enterprises, their WUE, and water withdrawal may change substantially over time, the broad spatial pattern after aggregating to grid scale
315



may still hold because the spatial pattern of IWW is largely determined by the distribution of population and economy of the country. Nevertheless, temporal changes in driving factors of IWW, such as industrial structure, water use efficiency, and climate, etc. (Alcamo et al., 2003; OTAKI et al., 2008; Flörke et al., 2013; Zhou et al., 2020), should be considered in future to achieve higher accuracy. Due to this limitation, CIWW data in earlier periods may contain larger uncertainty, and users should interpret it cautiously.

5 Conclusions

To fill the data gap in water withdrawal in China, one of the top water consumers in the world, we developed new gridded datasets, namely, the China Industrial Water Withdrawal Dataset. The dataset provided monthly IWW from 1965 to 2020 with a spatial resolution of 0.1° and 0.25°. With the best available data sources, the dataset presented significant improvements upon previous global datasets in characterizing the spatial pattern, seasonal variation, and long-term changes of IWW in China with a much higher accuracy. The transparent methodology and public availability of the source data allowed further adjustments and calibration to support the various applications by users. They also served as a reference for other countries to develop localized datasets of their own. The dataset could help understand the human water use dynamics and support studies in hydrology, geography, environment, sustainability sciences, and regional water resources management and allocation in China.

6 Data availability

The China Industrial Water Withdrawal Dataset is available at <https://doi.org/10.6084/m9.figshare.21901074.v1> (Hou and Li, 2023). The Database of Chinese Industrial Enterprises is available from the library resources of Peking University (<https://www.lib.pku.edu.cn/portal/cn/news/0000001637>). Chinese Economic Census Yearbook in 2008 is freely available to the public at <http://www.stats.gov.cn/tjsj/pcsj/jjpc/2jp/left.htm>. China Industry Product Output Database can be downloaded from the EPS data (<https://www.epsnet.com.cn/>). The provincial industrial water withdrawal data from 2003 to 2020 are from China Water Resources Bulletin (<http://www.mwr.gov.cn/sj/tjgb/szygb/>), while the data from 1965 to 2002 were obtained from Zhou et al., 2020 (<https://www.pnas.org/doi/10.1073/pnas.1909902117>).

340 Code availability

Python codes used in this study are available at GitHub (https://github.com/cch-yhm/CIWW_dataset)



Author contributions

Yan Li and Chengcheng Hou conceived and designed the study. Yinglu Liu and Chengcheng Hou contributed to data collection. Chengcheng Hou performed the data generation, data analysis and the original draft. Yan Li, Shan Sang, Xu Zhao, Yanxu Liu and Fang Zhao participated in reviewing and editing the paper. All authors have read and approved the paper.

Competing interests

The contact author has declared that none of the authors has any competing interests.

Financial support

This research is supported by the National Natural Science Foundation of China (no. 42041007, 41991235, and 72074136) and the Fundamental Research Funds for the Central Universities of China.

References

- Alcamo, J., Henrichs, T., and Rösch, T.: World Water in 2025 - Global modeling and scenario analysis for the World Commission on Water for the 21st Century, Kassel World Water Ser. 2, 47, 2000.
- Alcamo, J., Döll, P., Henrichs, T., Kaspar, F., Lehner, B., Rösch, T., and Siebert, S.: Development and testing of the WaterGAP 2 global model of water use and availability, *Hydrol. Sci. J.*, 48, 317–337, <https://doi.org/10.1623/hysj.48.3.317.45290>, 2003.
- Alcamo, J., Flörke, M., and Märker, M.: Future long-term changes in global water resources driven by socio-economic and climatic changes, *Hydrol. Sci. J.*, 52, 247–275, <https://doi.org/10.1623/hysj.52.2.247>, 2007.
- Arnell, N. W.: Climate change and global water resources, *Glob. Environ. Change*, 9, [https://doi.org/10.1016/S0959-3780\(99\)00017-5](https://doi.org/10.1016/S0959-3780(99)00017-5), 1999.
- Arnell, N. W.: Climate change and global water resources: SRES emissions and socio-economic scenarios, *Glob. Environ. Change*, 14, 31–52, <https://doi.org/10.1016/j.gloenvcha.2003.10.006>, 2004.
- Beek van, L. P. H., Wada, Y., and Bierkens, M. F. P.: Global monthly water stress: 1. Water balance and water availability: GLOBAL MONTHLY WATER STRESS, 1, *Water Resour. Res.*, 47, <https://doi.org/10.1029/2010WR009791>, 2011.
- Brunner, M. I., Zappa, M., and Stähli, M.: Scale matters: Effects of temporal and spatial data resolution on water scarcity assessments, *Adv. Water Resour.*, 123, 134–144, <https://doi.org/10.1016/j.advwatres.2018.11.013>, 2019.
- Byers, E. A., Hall, J. W., and Amezaga, J. M.: Electricity generation and cooling water use: UK pathways to 2050, *Glob. Environ. Change*, 25, 16–30, <https://doi.org/10.1016/j.gloenvcha.2014.01.005>, 2014.
- Chen, Y., Yin, G., and Liu, K.: Regional differences in the industrial water use efficiency of China: The spatial spillover effect and relevant factors, *Resour. Conserv. Recycl.*, 167, 105239, <https://doi.org/10.1016/j.resconrec.2020.105239>, 2021.



- 370 Derepasko, D., Peñas, F. J., Barquín, J., and Volk, M.: Applying Optimization to Support Adaptive Water Management of Rivers, *Water*, 13, 1281, <https://doi.org/10.3390/w13091281>, 2021.
- Flörke, M., Kynast, E., Bärlund, I., Eisner, S., Wimmer, F., and Alcamo, J.: Domestic and industrial water uses of the past 60 years as a mirror of socio-economic development: A global simulation study, *Glob. Environ. Change*, 23, 144–156, <https://doi.org/10.1016/j.gloenvcha.2012.10.018>, 2013.
- 375 Fujimori, S., Hanasaki, N., and Masui, T.: Projections of industrial water withdrawal under shared socioeconomic pathways and climate mitigation scenarios, *Sustain. Sci.*, 12, 275–292, <https://doi.org/10.1007/s11625-016-0392-2>, 2017.
- Gu, A., Teng, F., and Lv, Z.: Exploring the nexus between water saving and energy conservation: Insights from industry sector during the 12th Five-Year Plan period in China, *Renew. Sustain. Energy Rev.*, 59, 28–38, <https://doi.org/10.1016/j.rser.2015.12.285>, 2016.
- 380 Han, Z., Long, D., Fang, Y., Hou, A., and Hong, Y.: Impacts of climate change and human activities on the flow regime of the dammed Lancang River in Southwest China, *J. Hydrol.*, 570, 96–105, <https://doi.org/10.1016/j.jhydrol.2018.12.048>, 2019.
- Hanasaki, N., Kanae, S., Oki, T., Masuda, K., Motoya, K., Shirakawa, N., Shen, Y., and Tanaka, K.: An integrated model for the assessment of global water resources - Part 1: Model description and input meteorological forcing, *Hydrol. Earth Syst. Sci.*, 12, 1007–1025, <https://doi.org/10.5194/hess-12-1007-2008>, 2008a.
- 385 Hanasaki, N., Kanae, S., Oki, T., Masuda, K., Motoya, K., Shirakawa, N., Shen, Y., and Tanaka, K.: An integrated model for the assessment of global water resources - Part 2: Applications and assessments, *Hydrol. Earth Syst. Sci.*, 12, 1027–1037, <https://doi.org/10.5194/hess-12-1027-2008>, 2008b.
- Hanasaki, N., Inuzuka, T., Kanae, S., and Oki, T.: An estimation of global virtual water flow and sources of water withdrawal for major crops and livestock products using a global hydrological model, *J. Hydrol.*, 384, 232–244, <https://doi.org/10.1016/j.jhydrol.2009.09.028>, 2010.
- 390 Hejazi, M., Edmonds, J., Clarke, L., Kyle, P., Davies, E., Chaturvedi, V., Wise, M., Patel, P., Eom, J., Calvin, K., Moss, R., and Kim, S.: Long-term global water projections using six socioeconomic scenarios in an integrated assessment modeling framework, *Technol. Forecast. Soc. Change*, 81, 205–226, <https://doi.org/10.1016/j.techfore.2013.05.006>, 2014.
- Hou, C., Li, Y.: The China industrial water withdrawal Dataset (CIWW) —a gridded monthly industrial water withdrawal data in China from 1965 to 2020. figshare [data set], <https://doi.org/10.6084/m9.figshare.21901074.v1>, 2023.
- 395 Huang, Z., Hejazi, M., Li, X., Tang, Q., Vernon, C., Leng, G., Liu, Y., Döll, P., Eisner, S., Gerten, D., Hanasaki, N., and Wada, Y.: Reconstruction of global gridded monthly sectoral water withdrawals for 1971–2010 and analysis of their spatiotemporal patterns, *Hydrol. Earth Syst. Sci.*, 22, 2117–2133, <https://doi.org/10.5194/hess-22-2117-2018>, 2018.
- Koch, H. and Vögele, S.: Dynamic modelling of water demand, water availability and adaptation strategies for power plants to global change, *Ecol. Econ.*, 68, 2031–2039, <https://doi.org/10.1016/j.ecolecon.2009.02.015>, 2009.
- 400 Li, X., Long, D., Scanlon, B. R., Mann, M. E., Li, X., Tian, F., Sun, Z., and Wang, G.: Climate change threatens terrestrial water storage over the Tibetan Plateau, *Nat. Clim. Change*, <https://doi.org/10.1038/s41558-022-01443-0>, 2022.



- Liu, J., Zang, C., Tian, S., Liu, J., Yang, H., Jia, S., You, L., Liu, B., and Zhang, M.: Water conservancy projects in China: Achievements, challenges and way forward, *Glob. Environ. Change*, 23, 633–643, 405 <https://doi.org/10.1016/j.gloenvcha.2013.02.002>, 2013.
- Liu, L., Hejazi, M., Patel, P., Kyle, P., Davies, E., Zhou, Y., Clarke, L., and Edmonds, J.: Water demands for electricity generation in the U.S.: Modeling different scenarios for the water–energy nexus, *Technol. Forecast. Soc. Change*, 94, 318–334, <https://doi.org/10.1016/j.techfore.2014.11.004>, 2015.
- Liu, M., Fang, Y., and Li Y.: Analysis of Several Chinese National Economic Indexes’ Seasonal Fluctuation by Applying the 410 Methods of Directional Data Statistics, 64–72, 2006 (In Chinese).
- Liu, X., Tang, Q., Liu, W., Veldkamp, T. I. E., Boulange, J., Liu, J., Wada, Y., Huang, Z., and Yang, H.: A Spatially Explicit Assessment of Growing Water Stress in China From the Past to the Future, *Earths Future*, 7, 1027–1043, <https://doi.org/10.1029/2019EF001181>, 2019a.
- Liu, X., Liu, W., Yang, H., Tang, Q., Flörke, M., Masaki, Y., Müller Schmied, H., Ostberg, S., Pokhrel, Y., Satoh, Y., and 415 Wada, Y.: Multimodel assessments of human and climate impacts on mean annual streamflow in China, *Hydrol. Earth Syst. Sci.*, 23, 1245–1261, <https://doi.org/10.5194/hess-23-1245-2019>, 2019b.
- Long, D., Yang, W., Scanlon, B. R., Zhao, J., Liu, D., Burek, P., Pan, Y., You, L., and Wada, Y.: South-to-North Water Diversion stabilizing Beijing’s groundwater levels, *Nat. Commun.*, 11, 3665, <https://doi.org/10.1038/s41467-020-17428-6>, 2020.
- 420 Müller Schmied, H., Eisner, S., Franz, D., Wattenbach, M., Portmann, F. T., Flörke, M., and Döll, P.: Sensitivity of simulated global-scale freshwater fluxes and storages to input data, hydrological model structure, human water use and calibration, *Hydrol. Earth Syst. Sci.*, 18, 3511–3538, <https://doi.org/10.5194/hess-18-3511-2014>, 2014.
- Niva, V., Cai, J., Taka, M., Kummu, M., and Varis, O.: China’s sustainable water-energy-food nexus by 2030: Impacts of urbanization on sectoral water demand, *J. Clean. Prod.*, 251, 119755, <https://doi.org/10.1016/j.jclepro.2019.119755>, 2020.
- 425 Oki, T. and Kanae, S.: Global hydrological cycles and world water resources, *Science*, 313, 1068–1072, <https://doi.org/10.1126/science.1128845>, 2006.
- Oki, T., Agata, Y., Kanae, S., Saruhashi, T., and Musiake, K.: Global water resources assessment under climatic change in 2050 using TRIP, *IAHS-AISH Publ.*, 124–133, 2003.
- Otaki, Y., Otaki, M., and Yamada, T.: Attempt to Establish an Industrial Water Consumption Distribution Model, *J. Water 430 Environ. Technol.*, 6, 85–91, <https://doi.org/10.2965/jwet.2008.85>, 2008.
- Qin, J., Ding, Y.-J., Zhao, Q.-D., Wang, S.-P., and Chang, Y.-P.: Assessments on surface water resources and their vulnerability and adaptability in China, *Adv. Clim. Change Res.*, 11, 381–391, <https://doi.org/10.1016/j.accre.2020.11.002>, 2020.
- Qin, Y., Mueller, N. D., Siebert, S., Jackson, R. B., AghaKouchak, A., Zimmerman, J. B., Tong, D., Hong, C., and Davis, S. 435 J.: Flexibility and intensity of global water use, *Nat. Sustain.*, 2, 515–523, <https://doi.org/10.1038/s41893-019-0294-2>, 2019.



- Shen, Y., Oki, T., Utsumi, N., and Kanae, S.: Projection of future world water resources under SRES scenarios : water withdrawal / Projection des ressources en eau mondiales futures selon les scénarios du RSSE : prélèvement d ' eau Projection of future world water resources under SRES scenarios : wat, *Hydrol. Sci. J.*, 53, 11–33, <https://doi.org/10.1623/hysj.53.1.11>, 2010.
- 440 Sunkara, S. V. and Singh, R.: Assessing the impact of the temporal resolution of performance indicators on optimal decisions of a water resources system, *J. Hydrol.*, 612, 128185, <https://doi.org/10.1016/j.jhydrol.2022.128185>, 2022.
- Vassolo, S. and Döll, P.: Global-scale gridded estimates of thermoelectric power and manufacturing water use, *Water Resour. Res.*, 41, 1–11, <https://doi.org/10.1029/2004WR003360>, 2005.
- Vörösmarty, C. J., Green, P., Salisbury, J., and Lammers, R. B.: Global water resources: Vulnerability from climate change and population growth, *Science*, 289, 284–288, <https://doi.org/10.1126/science.289.5477.284>, 2000.
- 445 Wada, Y., Van Beek, L. P. H., Viviroli, D., Drr, H. H., Weingartner, R., and Bierkens, M. F. P.: Global monthly water stress: 2. Water demand and severity of water stress, *Water Resour. Res.*, 47, 1–17, <https://doi.org/10.1029/2010WR009792>, 2011a.
- Wada, Y., Beek, L. P. H. V., and Bierkens, M. F. P.: Modelling global water stress of the recent past : on the relative importance of trends in water demand and climate variability, 15, 3785–3808, <https://doi.org/10.5194/hess-15-3785-2011>, 2011b.
- 450 Wada, Y., Wisser, D., and Bierkens, M. F. P.: Global modeling of withdrawal, allocation and consumptive use of surface water and groundwater resources, *Earth Syst. Dyn.*, 5, 15–40, <https://doi.org/10.5194/esd-5-15-2014>, 2014.
- Wada, Y., Flörke, M., Hanasaki, N., Eisner, S., Fischer, G., Tramberend, S., Satoh, Y., Van Vliet, M. T. H., Yillia, P., Ringler, C., Burek, P., and Wiberg, D.: Modeling global water use for the 21st century: The Water Futures and Solutions (WFaS) initiative and its approaches, *Geosci. Model Dev.*, 9, 175–222, <https://doi.org/10.5194/gmd-9-175-2016>, 2016.
- 455 Wang, J., Zhong, L., and Long, Y.: Technical Note Baseline Water Stress: China, *World Resour. Inst. Tech. Note*, 1–16, 2016.
- WWAP (UNESCO World Water Assessment Programme). 2019. The United Nations World Water Development Report 2019: Leaving No One Behind. Paris, UNESCO.
- Xia, J., Ning, L., Wang, Q., Chen, J., Wan, L., and Hong, S.: Vulnerability of and risk to water resources in arid and semi-arid regions of West China under a scenario of climate change, *Clim. Change*, 144, 549–563, [https://doi.org/10.1007/s10584-016-](https://doi.org/10.1007/s10584-016-1709-y)
- 460 1709-y, 2017.
- Yan, D., Zhang, X., Qin, T., Li, C., Zhang, J., Wang, H., Weng, B., Wang, K., Liu, S., Li, X., Yang, Y., Li, W., Lv, Z., Wang, J., Li, M., He, S., Liu, F., Bi, W., Xu, T., Shi, X., Man, Z., Sun, C., Liu, M., Wang, M., Huang, Y., Long, H., Niu, Y., Dorjsuren, B., Gedefaw, M., Li, Y., Tian, Z., Mu, S., Wang, W., and Zhou, X.: A data set of distributed global population and water withdrawal from 1960 to 2020, *Sci. Data*, 9, 640, <https://doi.org/10.1038/s41597-022-01760-1>, 2022.
- 465 Yin, Y., Wang, L., Wang, Z., Tang, Q., Piao, S., Chen, D., Xia, J., Conradt, T., Liu, J., Wada, Y., Cai, X., Xie, Z., Duan, Q., Li, X., Zhou, J., and Zhang, J.: Quantifying Water Scarcity in Northern China Within the Context of Climatic and Societal Changes and South-to-North Water Diversion, *Earths Future*, 8, <https://doi.org/10.1029/2020EF001492>, 2020.
- Zhao, X., Liu, J., Liu, Q., Tillotson, M. R., Guan, D., and Hubacek, K.: Physical and virtual water transfers for regional water stress alleviation in China, *Proc. Natl. Acad. Sci. U. S. A.*, 112, 1031–1035, <https://doi.org/10.1073/pnas.1404130112>, 2015.



- 470 Zhou, F., Bo, Y., Ciais, P., Dumas, P., Tang, Q., Wang, X., Liu, J., Zheng, C., Polcher, J., Yin, Z., Guimberteau, M., Peng, S., Ottele, C., Zhao, X., Zhao, J., Tan, Q., Chen, L., Shen, H., Yang, H., Piao, S., Wang, H., and Wada, Y.: Deceleration of China’s human water use and its key drivers, Proc. Natl. Acad. Sci. U. S. A., 117, 7702–7711, <https://doi.org/10.1073/pnas.1909902117>, 2020.

Appendix A

475 **Table A1 Classification of sectors in data**

No.	Subsector	Sector	Notes
6	Coal Mining and Dressing	Mining industry	
7	Petroleum and Naturel Gas Extraction		
8	Ferrous Metals Mining and Dressing		
9	<u>Non-ferrous Metals Mining and Dressing</u>		No industrial enterprise data
10	Non-metal Minerals Mining and Dressing		
11	Other Mining		No monthly product output data, filled by average of mining sector
13	Food Processing	Manufacture	
14	Food Manufacture	industry	
15	Beverage Processing		
16	Tobacco Processing		
17	Textile Industry		
18	Apparel, Footwear & Caps Manufacture		
19	Leather, Furs, Down, and Related Products		
20	Processing of Timber, Manufacturing of Wood, Bamboo, Rattan, Palm & Straw Products		
21	Furniture Manufacturing		
22	Paper & Paper Products		
23	Printing, Reproduction of Recording Media		
24	Cultural, Educational, and Sports Articles		



25	Petroleum Processing and Coking	
26	Raw Chemical Materials	
27	Medicines Manufacturing	
28	Chemical fibers Manufacturing	
29	Rubber Manufacturing	
30	Plastics Manufacturing	
31	Non-metal Mineral Products	
32	Smelting and Pressing of Ferrous Metal	
33	<u>Smelting and Pressing of Non-ferrous Metal</u>	No industrial enterprise data
34	Metal Products	
35	General Machinery	
36	Special Machinery	
37	Transportation Equipment	
39	Electric Equipment and Machinery	
40	Electronic and Telecommunications Equipment	
41	Instruments, Meters, Cultural and Office Machinery	
42	Artwork and Other Manufacturing Products	
43	Waste Resources and Material Recycling and Processing	No monthly product output data, filled by average of manufacturing sector
44	Electricity and Heating Power Production and Supply	Electricity and Gas Production
45	Gas Production and Supply	and Supply
46	<u>Water Production and Supply</u>	Unused, not for industrial purpose Un used



Appendix B

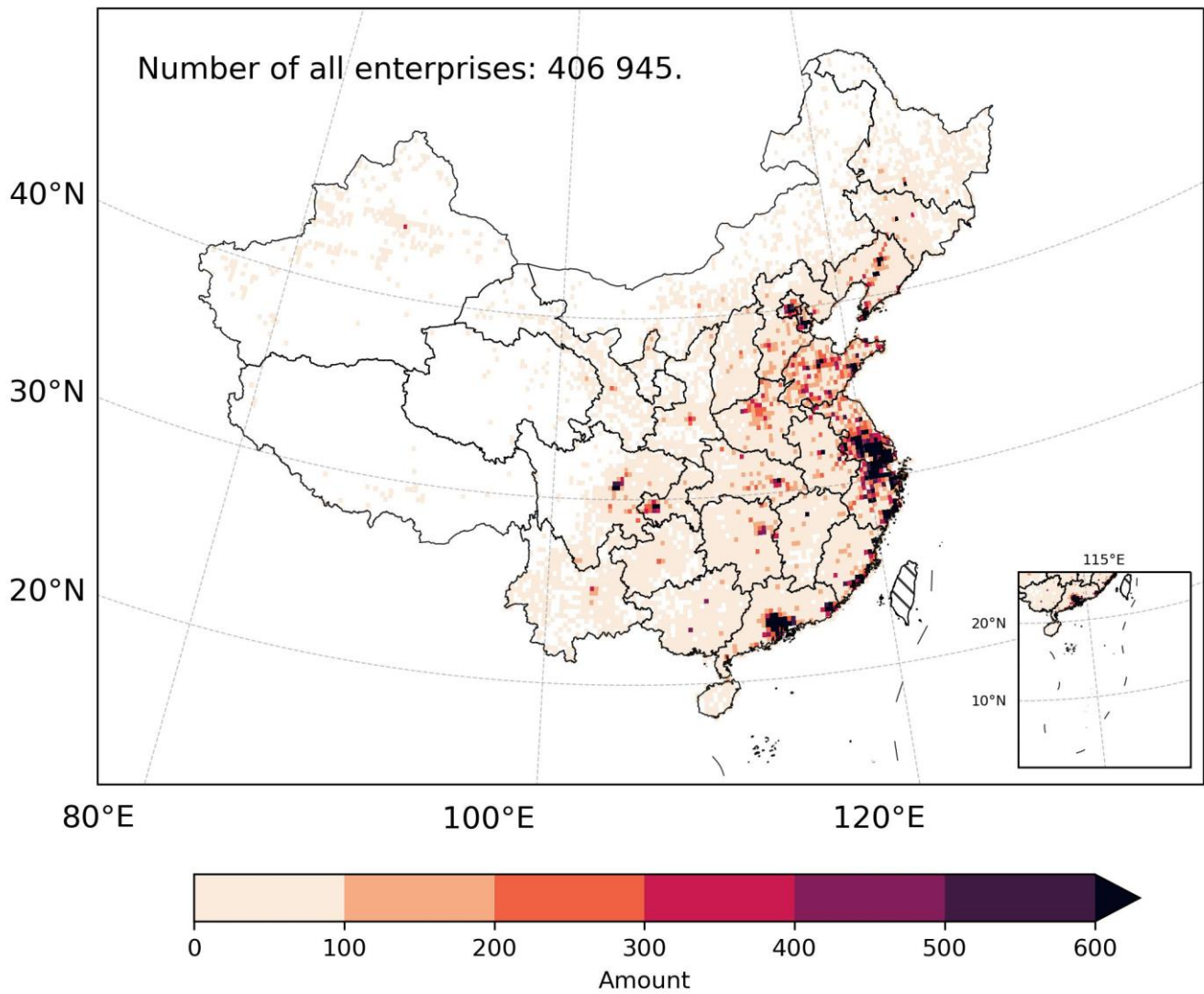


Figure B2: Spatial distribution of the number of industrial enterprises in China at 0.25°.



480 Appendix C

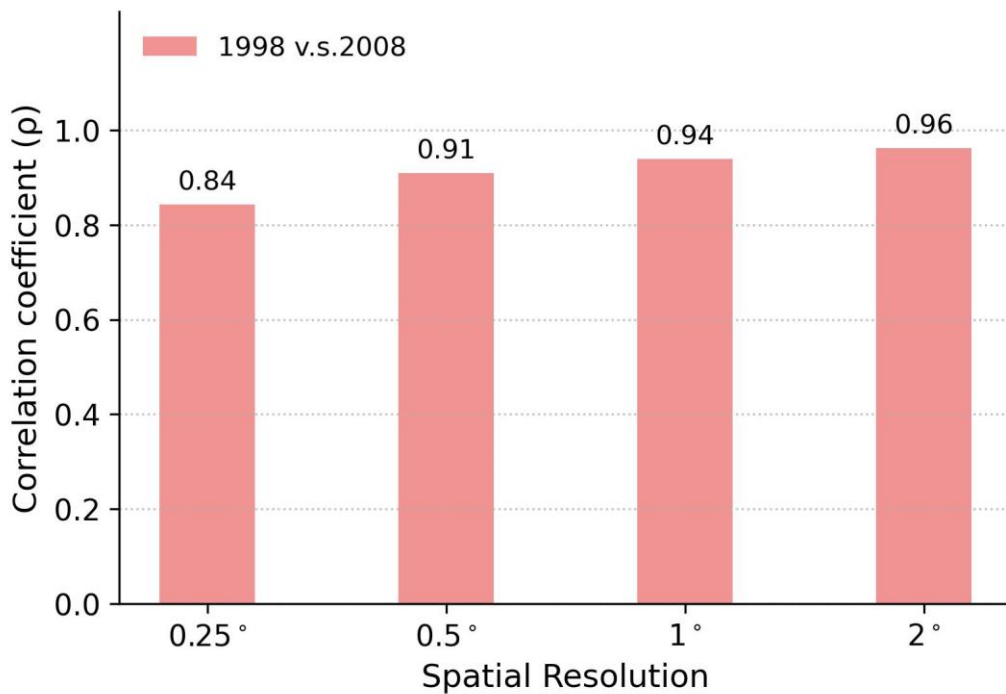


Figure C3: Spearman's rank correlation coefficients of the IWW spatial pattern between 1998 and 2008 at different spatial resolutions.

485